ISBN: 978-3-95450-232-5 ISSN: 2673-7000 doi:10.18429/JACoW-NAPAC2022-MOZE4

CERAMIC ENHANCED ACCELERATOR STRUCTURE LOW POWER TEST AND DESIGNS OF HIGH POWER AND BEAM TESTS*

H. Xu†, M. R. Bradley, M. A. Holloway, J. Upadhyay, L. D. Duffy
Los Alamos National Laboratory, Los Alamos, NM, USA

Abstract

A ceramic enhanced accelerator structure (CEAS) uses a concentric ceramic ring placed inside a metallic pillbox cavity to significantly increase the shunt impedance of the cavity. Single cell standing wave CEAS cavities are designed, built, and tested at low power at 5.1 GHz. The results indicate 40% increase in shunt impedance compared to that of a purely metallic pillbox cavity. A beam test setup has been designed to use a single cell CEAS cavity to modulate a 30 keV direct-current (DC) electron beam at an accelerating gradient of 1–2 MV/m to verify the beam acceleration capability of the CEAS concept and to study the potential charging effect on the ceramic component during the operation. Another single cell standing wave CEAS cavity has been designed for high power test at 5.7 GHz for the high accelerating gradient capability.

INTRODUCTION

In the designs of radiofrequency (RF) charged particle accelerators, low-loss ceramic components have been introduced as insertion in a variety of geometries with the purpose of reducing the power dissipation inside the structures, so as to enhance the shunt impedance of the accelerator cavities. Power saving achieved through the accelerator cavity shunt impedance enhancement is particularly desired in applications where the power availability is limited, e. g. space-borne experiments. However, due to the nature of ceramic material as dielectric and insulator, the main challenges of the applications of ceramic insertion in accelerator structures include the charging effects, multipactor, and the triple-point problem.

A ceramic enhanced accelerator structure (CEAS) was proposed to improve the shunt impedance of an accelerator cavity [1], as shown in Fig. 1. Inside an oxygen-free high thermal conductivity (OFHC) copper pillbox enclosure, a high-permittivity low-loss ceramic ring is positioned concentric with the metallic cell sidewall. A semi-loop coupler feeds microwave power into the region inside the ceramic ring. We investigated two types of the ceramic material, the BT37 ceramic (relative permittivity $\epsilon_r = 37.6$, loss tangent $\tan\delta = 2.75 \times 10^{-4}$) produced by Euclid Techlabs, LLC and the Skyworks 3500 series ceramic (relative permittivity $\epsilon_r = 34.5$, loss tangent $\tan\delta = 1.06 \times 10^{-4}$).

The cavity operates in a TM_{020} mode at 5.100 GHz. The radial distribution of the normalized longitudinal electric field and of the normalized azimuthal magnetic field is given in Fig. 2, calculated using the CST eigenmode solver for the CEAS geometry with the Euclid BT37 ceramic. The radial position of the ceramic ring overlaps with the node of the radial distribution of the longitudinal electric field. As a result, the dielectric loss inside the material of the ceramic ring is minimized, and the risk of direct dielectric breakdown is reduced as well. Because the ceramic ring possesses a high dielectric constant and thus is highly reflective, the magnitude of the fields in the region inside the ceramic ring is in general much greater than that beyond the ceramic ring. Therefore, the magnitude of the magnetic field at the metallic cell sidewall is very small, leading to reduced ohmic loss.

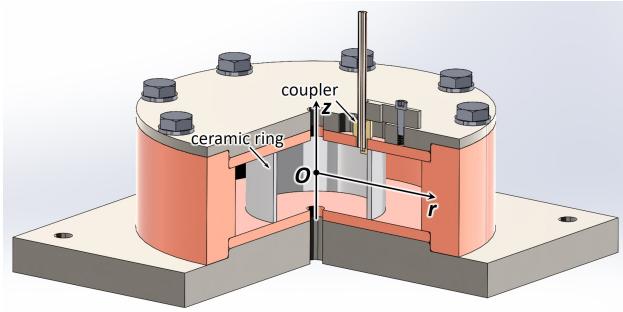

Figure 1: Section view of the low power test structure model of a ceramic enhanced accelerator structure (CEAS).

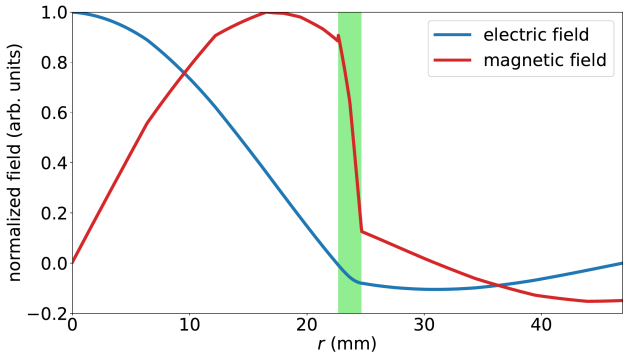

Figure 2: Radial distribution of the normalized longitudinal electric field and of the normalized azimuthal magnetic field at $z = 0$. The light green section represents the radial range of the ceramic ring made of the Euclid BT37 ceramic.

LOW POWER TEST

The goal of the low power test was to conduct the proof-of-principle verification of the CEAS concept, and to confirm the shunt impedance enhancement in a CEAS accelerator

* Work supported by the Laboratory Directed Research and Development program of Los Alamos National Laboratory, under project number 20210083ER.
† haoranxu@lanl.gov

ISBN: 978-3-95450-232-5 ISSN: 2673-7000 doi:10.18429/JACoW-NAPAC2022-MOZE4

cavity. The low power test standing wave cavity (Fig. 1) was designed to be a clamped structure, with the ceramic ring held in place by only the friction due to the clamping force. This plain geometry of the contact between the ceramic ring flat surfaces and the endplates does well in reducing the potential triple-point electric field enhancement.

The parts of the structure were fabricated by Jaguar Precision Machine, LLC. A vector network analyzer was used to measure the reflection coefficient (S_{11}) of the cavity, and to perform the measurement of the accelerating field profile. The measurements of the reflection coefficient and of the accelerating field profile were performed on the CEAS cavities using the Euclid BT37 and the Skyworks 3500 ceramics, and on a control cavity in a conventional purely metallic pillbox geometry operating in a TM_{010} mode.

The CST driven modal simulation prediction and the measurement of the reflection coefficient magnitude of the CEAS cavity using the Euclid BT37 ceramic ring are compared in Fig. 3 as an example. Overcoupling is achieved in this case with the semi-loop coupler capturing maximized magnetic field flux, indicating that the cavity is potentially capable of performing beam acceleration while maintaining sufficient RF power coupling.

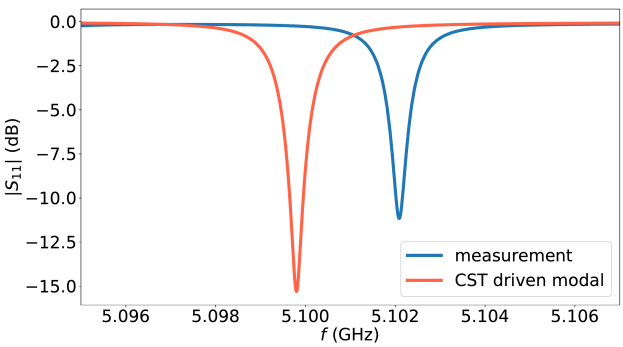

Figure 3: Comparison of the CST driven modal simulation and the low power test measurement results of the reflection coefficient magnitude of the CEAS cavity using the Euclid BT37 ceramic ring.

The on-axis accelerating field measurement was carried out using the non-resonant perturbation method, and the comparison of the CST eigenmode simulation and the low power measurement results are given in Fig. 4, showing good agreement.

The measured resonant frequency (f_0), intrinsic quality factor (Q_0), and time-independent shunt impedance per unit structure length (r_{sh}) are listed in Table 1. The results indicate that the resonant frequency of the CEAS cavity using the Skyworks 3500 ceramic was 18 MHz below the designed value. The Skyworks 3500 ceramic ring was fabricated as eight 45-degree segments to be assembled as a complete tube, due to the limited dimensions of the raw material available. The ceramic segments were machined at Los Alamos National Laboratory (LANL). Assembly errors caused the ceramic ring to have slightly greater inner and outer radii,

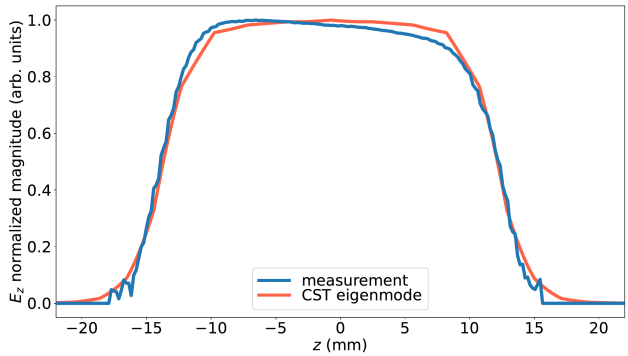

Figure 4: Comparison of the CST eigenmode simulation and the low power test measurement results of the on-axis accelerating field magnitude profile of the CEAS cavity using the Euclid BT37 ceramic ring.

leading to the measured resonant frequency below the designed value of 5.100 GHz.

Table 1: Measured RF Properties from the Low Power Test of the CEAS Cavities and the Control Pillbox Cavity

Cavity	f_0 (GHz)	Q_0	r_{sh} (MΩ/m)
CEAS - Euclid BT37	5.102	15664	199.7
CEAS - Skyworks 3500	5.082	18709	217.4
Conventional Pillbox	5.100	11135	154.8

Compared to the case of the conventional pillbox cavity, the shunt impedances of the CEAS cavities using the Euclid BT37 and the Skyworks 3500 ceramics are significantly higher, by 29% and 40%, respectively. With a given accelerating gradient, the CEAS cavities using the two types of ceramics tested are expected to accomplish RF power saving by 22% and 29%.

BEAM TEST DESIGN

The beam test is the next stage of the CEAS research. The purpose of the beam test is to verify the capability of CEAS accelerator structures in performing electron beam acceleration in realistic applications. The experimental design of the beam test setup for a CEAS cavity at 5.1 GHz using the Euclid BT37 ceramic was completed and is illustrated in Fig. 5.

A 30 kV 1-mA electron gun generates a direct current beam, which witnesses the accelerating field inside the CEAS cavity and gets modulated. The electron beam traverses a dipole that serves as an energy spectrometer downstream and is projected onto a phosphorous screen for the measurement of the energy modulation exerted by the CEAS accelerator cavity.

Because the electron beam is sub-relativistic, a set of nose cones are used in the design of the CEAS cavity for the beam test. The accelerator cavity is to be powered by a high-electron mobility transistor (HEMT) unit [2], and the expected accelerating gradient of the beam test cavity is

ISBN: 978-3-95450-232-5 ISSN: 2673-7000 doi:10.18429/JACoW-NAPAC2022-MOZE4

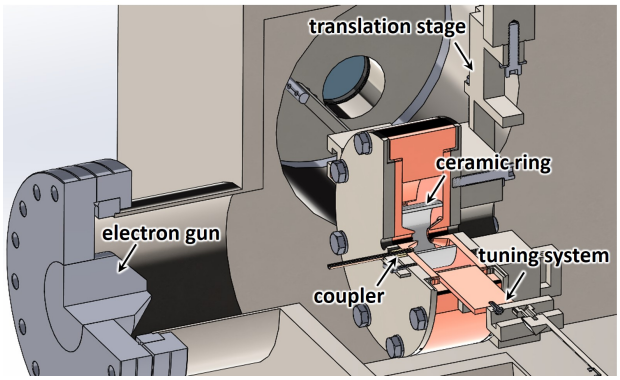

Figure 5: Beam test setup for the 5.1 GHz CEAS structure.

1–2 MV/m. At this level of the field magnitude, the ceramic ring needs to be brazed onto the copper endplates to avoid minuscule gaps between the ceramic ring and the endplates, which can cause electric field concentration, leading to dielectric breakdown. The research on the brazing technique is under way. The flat surfaces on both ends of an Euclid BT37 ceramic ring have been coated with copper at Acree Technologies Inc., and the ceramic-copper brazing research is in progress at IMG Altair, LLC.

In the beam test, the effects of the temperature rise and of the possible charging on the ceramic component will be studied. Two slab tuners positioned opposite to each other (Fig. 5) are used to tune the cavity as the temperature varies. The tuners are designed to achieve a tuning bandwidth of 5 MHz.

HIGH POWER TEST DESIGN

The motivation of the high power test of an CEAS cavity is to investigate the high accelerating gradient limit of the CEAS geometry, assisted with state-of-the-art technologies elaborating the ceramic insertion into an accelerator cavity. The high power test will be performed at the high gradient C-band test stand at LANL [3].

The CST driven modal simulations and the mechanical design of a 5.712 GHz single cell standing wave CEAS accelerator structure (Fig. 6) for the high power test were completed. High power microwave generated from a C-band klystron enters the structure through the circular waveguide, and on-axis accelerating field is established in the pattern of a π-mode in the input coupling, central, and output coupling cells, with the field magnitude ratio approximately 1:2:1. The CEAS geometry is applied only to the central cell. Two side slots are opened on the opposite sides of the central cell OFHC copper sidewall, for the purpose of gas molecule flow and of optical diagnostic for photon emission from dielectric breakdown as well as surface flashover.

As in the beam test structure, the ceramic ring will be coated and brazed onto the copper endplates to avoid electric field enhancement at the contact position of the ceramic ring to the endplates. To mitigate the electron multipactor, a diamond-like carbon (DLC) layer will be coated on the

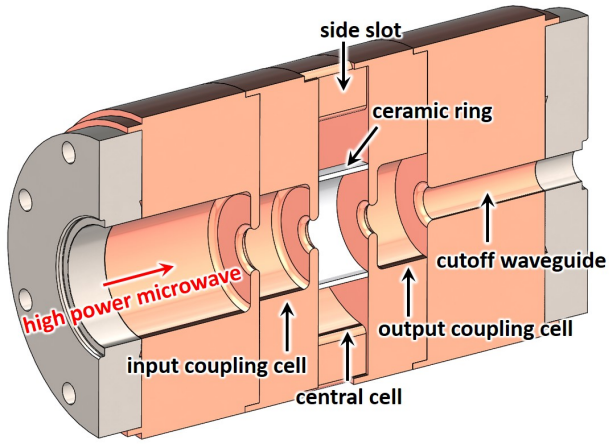

Figure 6: 5.712 GHz single cell standing wave CEAS cavity for high power test.

circular surfaces of the ceramic ring [4, 5], to reduce the secondary electron yield on the ceramic surface.

CONCLUSIONS

The concept of the ceramic enhanced accelerator structure (CEAS) for increasing the shunt impedance of an accelerator cavity has been verified at low power at 5.1 GHz using ceramic rings made of Euclid BT37 and of Skyworks 3500 ceramics. Improved shunt impedance in the CEAS accelerator structures results in RF power saving in charged particle accelerator applications.

CEAS structure beam test has been designed at 5.1 GHz to verify the electron beam acceleration capability of the cavity. The temperature rise due to structure power dissipation and potential ceramic charging effects will be studied.

CEAS structure high power test structure has been designed at 5.712 GHz to investigate the high accelerating gradient limit achievable in the cavity. Effects of microwave breakdown, electron multipactor, and ceramic surface flashover will be studied.

REFERENCES

[1] J. Upadhyay *et al.*, "Design of a ceramic enhanced normal conducting standing wave accelerator structure for higher shunt impedance," *Nucl. Instrum. Methods Phys. Res. A*, vol. 1034, no. 166669, 2022. doi:10.1016/j.nima.2022.166669

[2] J.W. Lewellen *et al.*, "Space-Borne Electron Accelerator Design," *Front. Astron. Space Sci.*, vol. 6, pp. 35, 2019. doi:10.3389/fspas.2019.00035

[3] E.I. Simakov, "New accelerator capabilities with the high-gradient C-band," LA-UR-21-30757, Los Alamos National Laboratory, Los Alamos, NM, USA, 2021.

[4] H. Xu *et al.*, "Measurement of internal dark current in a 17 GHz, high gradient accelerator structure," *Phys. Rev. Accel. Beams*, vol. 22, no. 021002, 2019. doi:10.1103/PhysRevAccelBeams.22.021002

[5] S. Mori *et al.*, "Multipactor suppression in dielectric-assist accelerating structures via diamondlike carbon coatings," *Phys. Rev. Accel. Beams*, vol. 24, no. 022001, 2021. doi:10.1103/PhysRevAccelBeams.24.022001